SEMARAK ILMU PUBLISHING

CFD Letters

Journal homepage: https://semarakilmu.com.my/journals/index.php/CFD_Letters/index
ISSN: 2180-1363

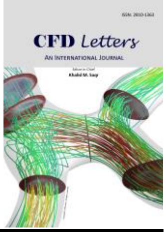

The Properties of the Physical Parameters in the Triple Diffusive Fluid Flow Model

Siti Suzilliana Putri Mohamed Isa[1,2*], Nanthini Balakrishnan[1], Kartini Ahmad[3], Norihan Md. Arifin[1,4], Fadzilah Md Ali[1,4]

[1] Institute for Mathematical Research, Universiti Putra Malaysia, 43400 UPM Serdang, Selangor Darul Ehsan, Malaysia
[2] Centre for Foundation Studies in Science of Universiti Putra Malaysia, Universiti Putra Malaysia, 43400 UPM Serdang, Selangor Darul Ehsan, Malaysia
[3] Department of Science in Engineering, Kuliyyah of Engineering, International Islamic University Malaysia, 50728 Gombak, Kuala Lumpur, Malaysia
[4] Department of Mathematics, Faculty of Science, Universiti Putra Malaysia, 43400 UPM Serdang, Selangor Darul Ehsan, Malaysia

ARTICLE INFO

Article history:
Received 1 November 2023
Received in revised form 5 December 2023
Accepted 9 January 2024
Available online 30 June 2024

Keywords:
Local Nusselt number; local Sherwood number; triple diffusive

ABSTRACT

The existence of more than one diffusive component in fluid mixtures is observed in these situations: underground water flow, the mechanism of acid rain, the existence of contaminant in some certain mixture, etc. These diffusive components are occurred with the single temperature gradient (since all of the elements are dissolved into the same mixture) and 2 types of concentration gradients (since the dual diffusive components are dissolved in the same mixture). Besides, many industrial and engineering processes are utilizing the concept of convective fluid flow especially over a shrinking sheet. Therefore, a mathematical model for triple-diffusive flow over a nonlinear compressing sheet has been developed in this paper, and subjected to the Soret-Dufour effects. The model comprises of five initial equations namely continuity, momentum, energy, concentration of component 1 and concentration of component 2 equations, together with boundary conditions. These initial equations are expressed as partial differential equations. However, the finalized equations are in the form of ordinary differential equations. Later, the bvp4c programme provided by the Matlab Software is used to solve the ordinary differential equations and the boundary conditions. Three distinct values of each governing parameter are fixed into the bvp4c function, to observe the behaviour of the physical parameters, namely as local Nusselt number and local Sherwood number. The main finding of the dual numerical solutions varies for increasing governing parameters until they intersect at the critical points. In conclusion, the governing parameters affects the heat and mass transfer of the fluid flow model model.

1. Introduction

Newtonian fluid is seen from its property whose viscosity is unaffected by shear rate. As such, it has the simplest mathematical model in which the viscosity term is taken into calculation. Whilst the non-Newtonian fluids cover broader spectrum of fluids which make them more practical in industrial

* Corresponding author.
E-mail address: ctsuzilliana@upm.edu.my (Siti Suzilliana Putri Mohamed Isa)

https://doi.org/10.37934/cfdl.16.11.133145

applications, the underlying of Newtonian fluid is of great importance. Ludwig Prandtl proved in his study of Newtonian fluids that viscosity plays its role in the fluid boundary layer, while viscosity can be neglected in the region around or outside the fluid boundary [1]. Some of the early works can be found in Ref. [2-4].

The interest of fluid flow over an extending sheet has gained substantial attention in view of several industrial applications such as the extrusion of plastic sheets from a die, cooling of continuous strips, glass fibre production and etc. The boundary layer flow due to an extending sheet can be occurred to the various types of fluid (Newtonian or non-Newtonian fluid). Sakiadis [5] was the first to venture the study of extending sheet which later motivates others to further explore the same scope. Subsequently, the related studies are developed with the additional restrictions such as affected by joule heating and viscous dissipation [6], the mixed convection model [7], and bounded by a permeable medium [8]. The fluid types are Newtonian [6] and non-Newtonian Casson fluid [7,8]. On contrary, the effect of compressing sheet was considered by previous studies [9-11] for the ferrofluids [9], Newtonian fluid [10], and hybrid nanofluid [11].

All the above mentioned studies considered the motion of fluid on a flat surface. It is worth noting that motion of fluid flow can also be along inclined surfaces. The inclined extending model in the Newtonian [12] and non-Newtonian fluid have been reported [13,14] recently. The characteristics of these studies are as follow: The magnetohydrodynamics (MHD) Newtonian model [12], water-based nanofluid with gyrotactic micro-organism [13], and a electrification of particles in a dusty flow [14].

The imposition of radiation in the boundary layer fluid flow is very significant especially when the temperature difference between the sheet and the ambient is extremely high. This in turn results in various industrial applications such as combustion of fuels, gas turbine, nuclear power stations, operation of a furnace and etc. The radiating fluid flow over an inclined sheet has been described due to the specific characteristics such as when the MHD Williamson nanofluid is affected by a non-uniform heat source/sink [15], when the convection model is unsteady and the interaction among the dissolved particles are taking into account [16], and the nanoparticles in the water are copper and alumina in the mixed convection nanofluid model [17].

All the above reported references do not incorporate mass and heat fluxes. Whenever there are composition and temperature gradients, energy and mass fluxes will be produced in the boundary layer fluid flow model. These are known to be Dufour and Soret effects, respectively and these features have been reported recently [18-20]. These publications described the effect of the heat source and first order chemical reaction in the Casson fluid [18], the boundary layer fluid flow when the boundary shape of the fluid is an inclined square enclosure [19], and the Casson fluid flow model is subjected to the thermal radiation and heat source/sink [20].

Triple diffusive in the fluid flow is formed when there are simultaneous differences in these three components: temperature, salinity, and the concentration of the certain particles submerged in the fluid. The triple diffusive model can be implemented in the industrial applications, such as in metal casting and alloy production, chemical engineering, hydrothermal vent system, etc. The recent studies regarding the triple diffusive flow are reported, based on the variations of heat source and temperature gradients [21-23], and magneto-convection system [24,25].

Motivated by the above mentioned works, this study is dedicated to the fluid flow over an inclined stretching sheet under several physical properties such as radiation and Soret-Dufour effects, and under the model of triple diffusive as reported by Archana *et al.,* [26]. They reported the properties of triple diffusive convection in an incompressible nanoliquid and bounded by horizontal flat surface. Their model is innovated in this paper by changing the boundary surface to be inclined, and the original fluid from the previous model which is nanofluid is replaced by Newtonian fluid. The triple diffusive mathematical model is developed in this paper and Archana *et al.,* [26] since it can describe the properties of heat and mass diffusion, simultaneously.

2. Methodology
2.1 Flow Model

The diagram of the fluid model is presented in Figure 1, and characteristics of the fluid flow model are as below:

i. The dimension in this model is two-dimensional Cartesian coordinates
ii. The Newtonian fluid (water) acts as a based fluid which contain 2 different components: Sodium chloride (NaCl) and sucrose with respecting concentrations C_1 and C_2.
iii. The temperature and concentration at the sheet are denoted by T_w, C_{1w} and C_{2w}, where the location at the sheet for the temperature and concentration variations is denoted as subscript w. The subscript 1 in the concentration C_{1w} is referred to the concentration of the first component, whereas the subscript 2 in C_{2w} defines the concentration of the second component.
iv. Otherwise, the ambient temperature and solutal concentrations are represented by T_∞, $C_{1\infty}$ and $C_{2\infty}$. The subscript ∞ in for these symbols (T_∞, $C_{1\infty}$ and $C_{2\infty}$) is indicated by the location of the fluid point far from the sheet. The subscript 1 in $C_{1\infty}$ is indicated as the concentration of the first component, whereas the subscript 2 in $C_{2\infty}$ defines the concentration of the second component.
v. The fluid is bounded by a compressing sheet, where this sheet is projected by a certain angle α from a reference axis.
vi. The velocity in horizontal and vertical axes is denoted by p and q. The velocity of the compressing sheet is represented by p_w whereas the wall mass suction is indicated by $q_w < 0$.

2.2 Continuity Equation

The continuity equation is shown as below:

$$p_x = -q_y \tag{1}$$

The velocity components p and q are represented based from the stream function$\psi = \alpha {R_{ax}}^{1/4}$, where $p = \psi_y$ and $q = -\psi_x$. The boundary layer thickness is denoted as η.

$$\begin{aligned} \psi &= \alpha {R_{ax}}^{1/4} \\ R_{ax} &= \frac{g(1 - C_\infty)\beta_T (T_w - T_\infty) x^3}{\nu\alpha} \\ \eta &= {R_{ax}}^{1/4} \frac{y}{x} \end{aligned} \tag{2}$$

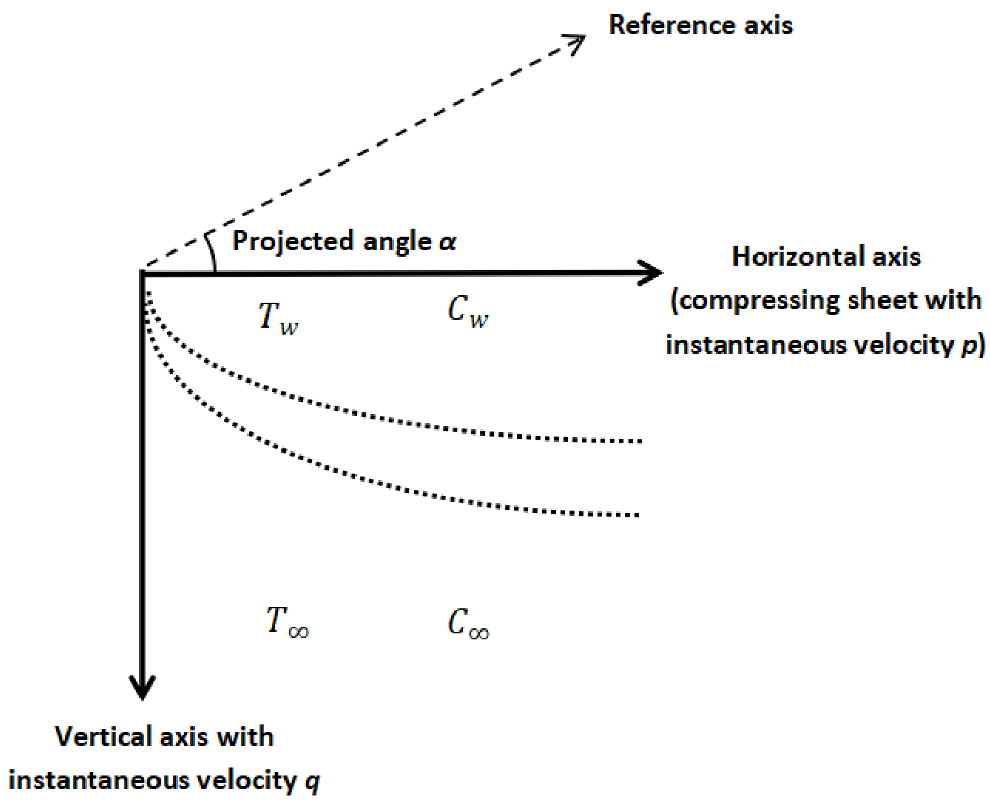

Fig. 1. The graphical representation of the fluid flow model

Substitute Eq. (2) into Eq. (1), then Eq. (1) is satisfied.

2.3 Momentum Equation

The momentum equation for this model is

$$\rho_f(pp_x + qp_y) = \mu p_{yy} - \left\{(1 - C_\infty)\rho_{f\infty}\begin{bmatrix}\beta_T(T - T_\infty) + \beta_{C1}(C_1 - C_{1\infty}) \\ +\beta_{C2}(C_2 - C_{2\infty})\end{bmatrix}\cos\alpha\right\}g \tag{3}$$

Where ρ_f is the fluid density, μ is the fluid viscosity coefficient, β_T is the coefficient of thermal expansion, β_C is the coefficient of volumetric solutal expansion of component 1 and component 2 respectively, and g is the gravitational acceleration.

The following similarity variables are introduced to transform the partial differential equations into ordinary differential equations.

$$T = T_\infty[1 + (\theta_w - 1)\theta(\eta)],$$
$$\theta(\eta)=\frac{T-T_\infty}{T_w-T_\infty}, \qquad \phi_1(\eta)=\frac{C_1-C_{1\infty}}{C_{1w}-C_{1\infty}}, \qquad \phi_2(\eta)=\frac{C_2-C_{2\infty}}{C_{2w}-C_{2\infty}} \tag{4}$$

Substituting Eq. (2) and Eq. (4) into Eq. (3), then Eq. (3) is transformed as:

$$f_{\eta\eta\eta} + \frac{1}{4Pr}\left(3ff_{\eta\eta} - 2(f_\eta)^2\right) - (\theta + N_{C1}\varphi_1 + N_{C2}\varphi_2)\cos\alpha = 0 \tag{5}$$

Here, Pr is the Prandtl number and N_C is the buoyancy ratio parameter where the subscripts 1 and 2 refer to the NaCl and sucrose. Pr is defined as the ratio of momentum diffusivity to thermal diffusivity, whereas N_C indicates the relative strength of the natural convection to the forced convection.

2.4 Energy Equation

The representation of the energy equation is shown by Eq. (6):

$$pT_x + qT_y = aT_{yy} + \tau\left[\frac{D_T}{T_\infty}\left(T_y\right)^2\right] - \frac{1}{(\rho c)_f}(q_r)_y + D_{TC1}(C_1)_{yy} + D_{TC2}(C_2)_{yy} \quad (6)$$

Where $a = k/(\rho c)_f$ is the thermal diffusivity of the fluid, k is the thermal conductivity, c_f is the specific heat coefficient of fluid, $\tau = (\rho c)_p/(\rho c)_f$ is the ratio of effective heat capacity of the nanoparticle material to heat capacity of the fluid, D_T is the coefficient of thermophoretic diffusion, q_r is the radiative heat flux, D_{TC} is the Dufour type of diffusivity.

The final energy equation is

$$\begin{aligned}&\{1 + Rd[1 + (\theta_w - 1)\theta]^3\}\theta_{\eta\eta} + \frac{3}{4}\theta_\eta f + N_t\left(\theta_\eta\right)^2 + Db_1(\varphi_1)_{\eta\eta} + Db_2(\varphi_2)_{\eta\eta} \\ &+3Rd[1 + (\theta_w - 1)\theta]^2(\theta_w - 1)\left(\theta_\eta\right)^2 = 0\end{aligned} \quad (7)$$

Where Rd is the radiation, θ_w is the temperature ratio, N_t is the thermophoresis and Db is the Dufour number. Rd indicates the relative contribution of conduction heat transfer to thermal radiation transfer, N_t defines the force induced a temperature gradient, and Db defines the effect of the concentration gradients to the thermal energy transfer.

2.5 Concentration Equation

The concentration of 2 components are

$$p(C_1)_x + q(C_1)_y = D_{s1}(C_1)_{yy} + D_{C1T}T_{yy} \quad (8)$$

$$p(C_2)_x + q(C_2)_y = D_{s2}(C_2)_{yy} + D_{C2T}T_{yy} \quad (9)$$

By substituting the similarity variables Eq. (2) and Eq. (4) into Eq. (8)-(9), then these equations become

$$\phi_{1_{\eta\eta}} + \frac{3}{4}Le_1 f\phi_{1_\eta} + Sr_1\theta_{\eta\eta} = 0 \quad (10)$$

$$\phi_{2_{\eta\eta}} + \frac{3}{4}Le_2 f\phi_{2_\eta} + Sr_2\theta_{\eta\eta} = 0 \quad (11)$$

Where Le and Sr is the Lewis number and Soret number, respectively. Le is defined as the ratio of thermal diffusivity to mass diffusivity. Besides, Sr shows the result of the concentration distribution induced by a temperature gradient.

2.6 Boundary Conditions

The restrictions at the boundaries are stated as

$$\begin{array}{llllll} p = \lambda\alpha A^{1/2}x^{1/2}, & q = q_w, & T = T_w, & C_1 = C_{1w}, & C_2 = C_{2w} & \text{at } \ y = 0, \\ p \to 0, & q \to 0, & T \to T_\infty, & C_1 \to C_{1\infty}, & C_2 \to C_{2\infty} & \text{as } \ y \to \infty. \end{array} \tag{12}$$

The compressing sheet parameter is denoted by $\lambda < 0$. The wall mass suction velocity, $q_w(x) < 0$ and L refers to the reference length of the compressing inclined sheet.

Above equation is transformed as below, by using Eq. (2) and Eq. (4):

$$\begin{array}{llllll} f_\eta = \lambda, & f = S, & \theta(0) = 1, & \varphi_1(0) = 1, & \varphi_2(0) = 1 & \text{at } \ \eta = 0, \\ f_\eta \to 0, & f \to 0, & \theta(\infty) \to 0, & \varphi_1(\infty) \to 0, & \varphi_2(\infty) \to 0 & \text{as } \ \eta \to \infty. \end{array} \tag{13}$$

where $S > 0$ is the suction parameter.

2.7 Physical Parameters for the Heat and Mass Transfers

The physical parameters helps to understand how the fluid flow, heat and mass transfer behaves on the surface of the stretching sheet. It is important to explore the effects that the governing parameters will leave on these parameters in order to have the knowledge about the fluid dynamics on the surface. In this study, two physical parameters are considered. The local Nusselt number and local Sherwood number for the both components are defined as below,

$$Nu_x = [x/k(T_w - T_\infty)]\left(-k\frac{\partial T}{\partial y} + (q_r)_w\right)_{y=0} \tag{14}$$

$$Sh_{x1} = [x/(C_{1w} - C_{1\infty})]\left(-\frac{\partial C_1}{\partial y}\right)_{y=0} \tag{15}$$

$$Sh_{x2} = [x/(C_{2w} - C_{2\infty})]\left(-\frac{\partial C_2}{\partial y}\right)_{y=0} \tag{16}$$

The non-dimensional form of the physical parameters is obtained by substituting Eq. (2) and Eq. (4) into Eq. (14)-(16), and then the below equations are formed.

$$R_{ax}{}^{-1/4}Nu_X/\left(1 + Rd\theta_w{}^3\right) = -\theta'(0), \qquad R_{ax}{}^{-1/4}Sh_{x1} = -\phi_1{}'(0). \tag{17}$$
$$R_{ax}{}^{-1/4}Sh_{x2} = -\phi_2{}'(0).$$

From Eq. (17), the symbols Nu_x, Sh_{x1} and Sh_{x2} are included in the main parameters $-\theta'(0)$, $-\phi_1{}'(0)$, and $-\phi_2{}'(0)$, respectively. In the subsequent sections, the local Nusselt number, local Sherwood number for NaCl and local Sherwood number for sucrose are recognized as $-\theta'(0)$, $-\phi_1{}'(0)$, and $-\phi_2{}'(0)$, separately.

3. Results and Discussion

The aim of the current model is to numerically solve the triple diffusive convection in an incompressible Newtonian fluid and bounded by an inclined compressing surface. With the usage of Matlab bvp4c, the graphs of local Nusselt number and local Sherwood number have been drawn. Dual numerical solutions are found for all the graphical results in this study (Figures 2-5): First solution is drawn as a upper branch of the physical parameters (dashed line) and second solution (lower branch in the same graphs and is it sketched as a solid line). However, only the first solution is considered stable and physically reliable in the actual fluid situation [27-29]. The parametric values in this model are as follows: $\alpha = 60°$, $\mathrm{Pr} = 1$, N_t=0.1, N_{c1}=0.5, N_{c2}=0.1, $\mathrm{Rd} = 10$, Le_1=0.5, Le_2=0.7, and λ = 0.8. All these values can produce the numerical results that follows the boundary conditions, as presented in Eq. (13).

Before discussing the results from this mathematical model, the verification from the previous study has to be described. Therefore, this model has been compared with another type of numerical method, namely as shooting method. This specific method for the triple diffusive case has been described in details [30], hence only the comparison table (Table 1) is displayed in this paper for the single solution only (stable numerical solution). Table 1 displays the good comparison in the heat transfer rate, proves that the current method (bvp4c function provided by MATLAB software) is applicable to implement to perform the numerical results in this triple diffusive model.

Table 1
The heat transfer rate between Matlab bvp4c and shooting method

Compressing rate λ	MatLab bvp4c	Shooting method
-0.2	0.329666623	0.32957
-0.3	0.323023345	0.32301
-0.35	0.268465753	0.26832

Eq. (8)-(11), Eq. (13) and Eq. (17) are solved in the Matlab bvp4c method. The values of governing parameters, namely as buoyancy ratios of both components, thermophoresis parameter, Dufour number of both components, Lewis number for both components, radiation parameter, and Soret number for both components will be fixed in bvp4c function, together with the highest boundary layer thickness. These values, are accepted as long as the numerical results satisfy the boundary conditions. The physical parameters that have been reported in this paper are the local Nusselt number and local Sherwood number for component 1 and component 2, due to the effect of Soret and Dufour numbers.

3.1 Variations of Local Nusselt Number

It is important to study this variation in order to detect how much heat is being transferred by convection and how much is being transferred by conduction. Figures 2 and 3 are the graphs against Sr_1 and Sr_2 for increasing values of Db_1 and Db_2. The first and second solution of behave in opposite manner and intersect at the critical points as Sr_1 increases. The graphs decline for increasing value of Db_1 . This emphasizes that the more the heat transferred by concentration difference of component 1, the less the heat will be transferred by convection. In addition, the position of the critical point shows the region or the range of the stable or unstable solution. The critical points for Db_1=0.2, 0.4, 0.6 are 0.4648, 0.4761 and 0.4884 respectively. The critical points move to the right which shows that the greater value of Sr_1 is needed to make the first and second solutions equal as Db_1 increases.

The Soret parameter for component 2 also affects the profile of local Nusselt number in same manner as of component 1. For increasing value of Sr_2, the second solution of the profile increases while the first solution decreases until both solutions meet at one point. In Figure 3, when Db_2 is increased, both the solutions decline. These two solutions meet at the critical points Sr_{2c} = 1.0420, 1.0275, 0.9870. Unlike component 1, for component 2, the critical points are decreasing. These values clearly show that for greater value of Db_2, the solutions intersect at small value of Sr_2.

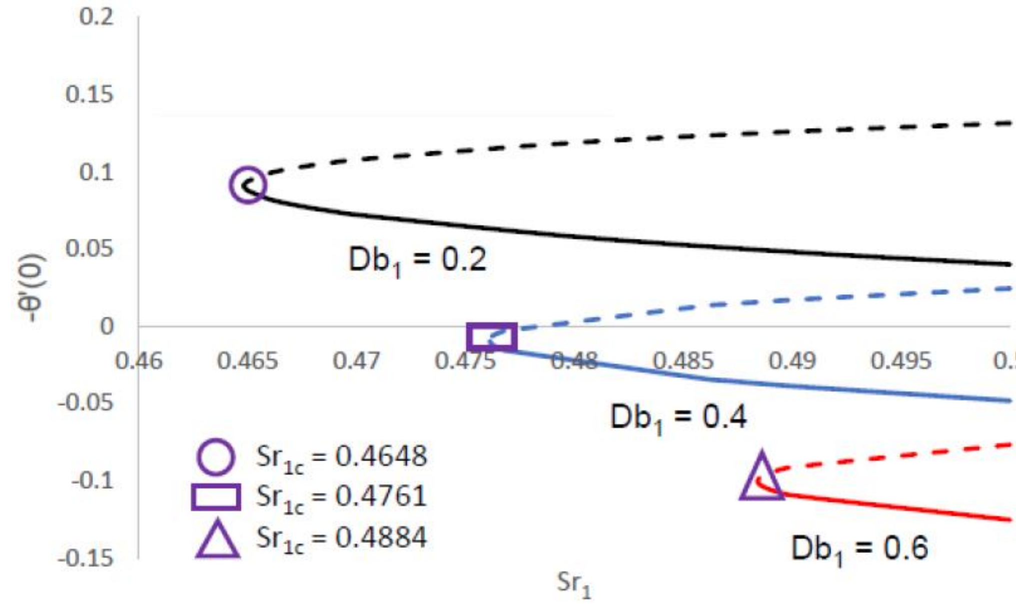

Fig. 2. The variation of local Nusselt number against Sr_1 for different values of Db_1

From Figure 2, the largest range of the local Nusselt number for NaCI is owned by the numerical solution obtained by Db_1=0.2 and Sr_{1c}= 0.4648. On the other hand, the largest range of the local Nusselt number for the sucrose (Figure 3) is when Db_2=1.0 and Sr_{2c}= 1.0420. As a result, the highest range of numerical solution of the local Nusselt number can be obtained for the lowest Dufour number.

The variations of the local Nusselt number (Figures 2 and 3) show that the region of the numerical solution is largest for the lowest Dufour number. This observation indicates that the heat transfer is affected by some range of the Soret number and to archieve a maximum range of heat transfer, the lowest Dufour number must be selected in the mathematical model. Besides, since the local Sherwood number can be expanded when the Dufour number is high, the range of the mass transfer can be extended by the high value of Dufour number.

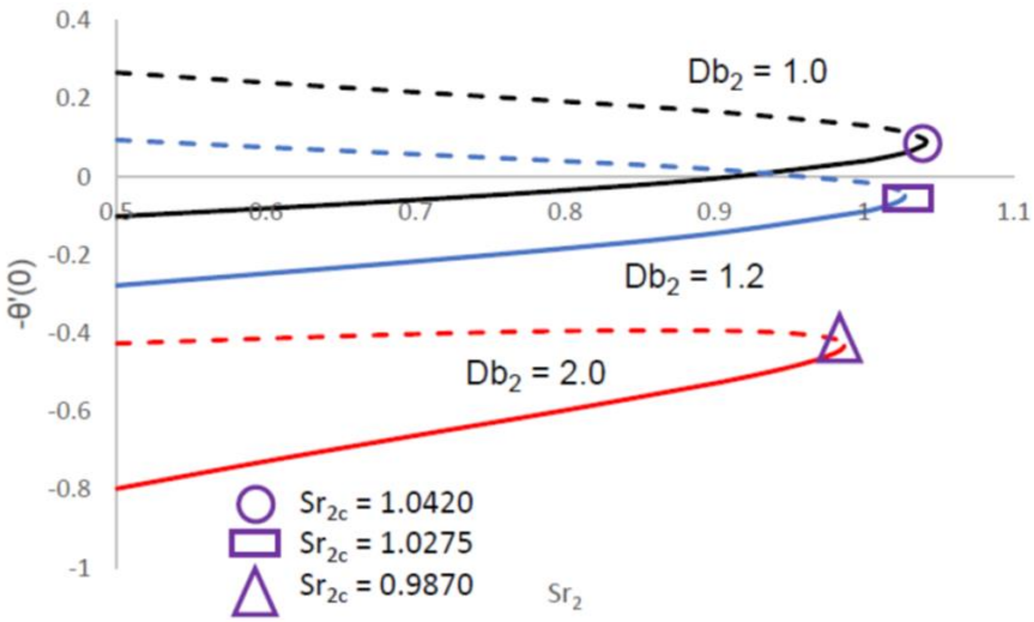

Fig. 3. The variation of local Nusselt number against Sr_2 for different values of Db_2

3.2 Variations of Local Sherwood Number

In triple diffusive flow, the mass of fluid is transferred according to temperature and concentration gradient by both convection and diffusion. It is very crucial to study about how much of mass is actually being transferred by convection and how much is being transferred by diffusion along the surface of compressing sheet which is actually the local Sherwood number. The related studies regarding to the combination of heat-mass transfer, together with the numerical results of local Sherwood number have been reported [31-33]. The related graph against Sr_1 is illustrated in Figure 4. It could be observed that as the value of Db_1 increases, both the solutions rise. The critical points are moving to the right from 0.4648 to 0.4884.

In Figure 5, the values of local Sherwood number of component 2 is plotted against the increasing value of Sr_2. Like the previous profile, both solutions of this profile also rise for increasing value of Db_2. In addition, the critical values are moving to the left from 1.042 to 0.987 with increment in the parameter.

An increment in Dufour parameter means the decrement in the molecular diffusion. Thus, less mass of fluid is being transferred by diffusion which in return makes the value of Sherwood numbers to be large. This means that the mass of fluid being transferred by convection could be increased by increasing the value of Dufour parameters.

Both of the local Sherwood number graphs (Figures 4 and 5) show the largest range of stable and unstable numerical solution for the lowest Dufour number, by observing the position of the critical number of Soret number. Besides, the smallest region of the numerical solution is obtained when the Dufour number is the highest.

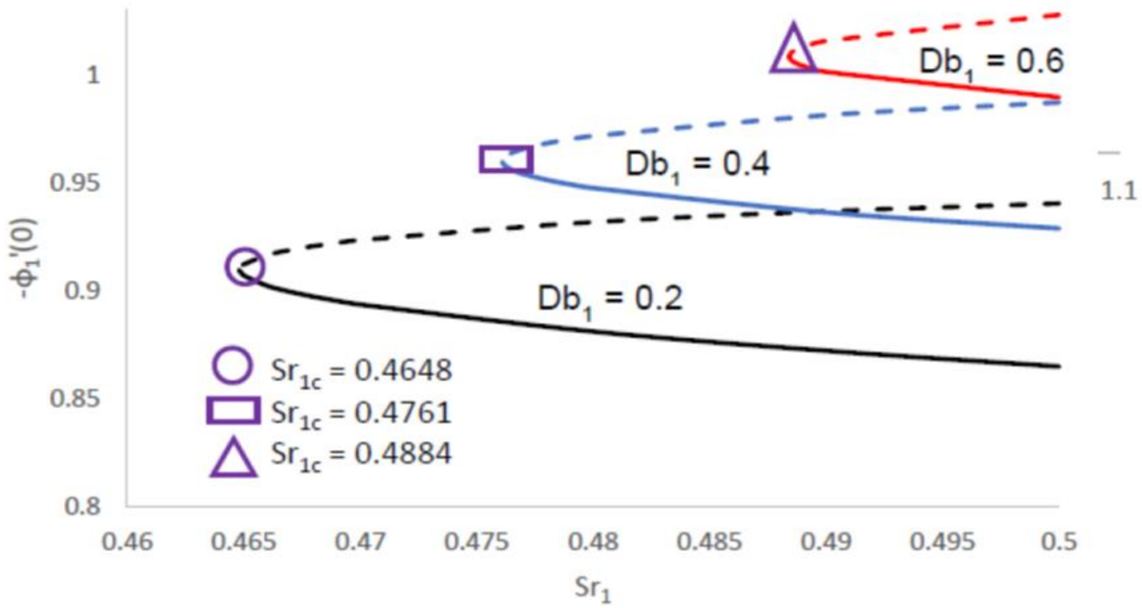

Fig. 4. The variation of local Sherwood number of component 1 against Sr_1 for different values of Db_1

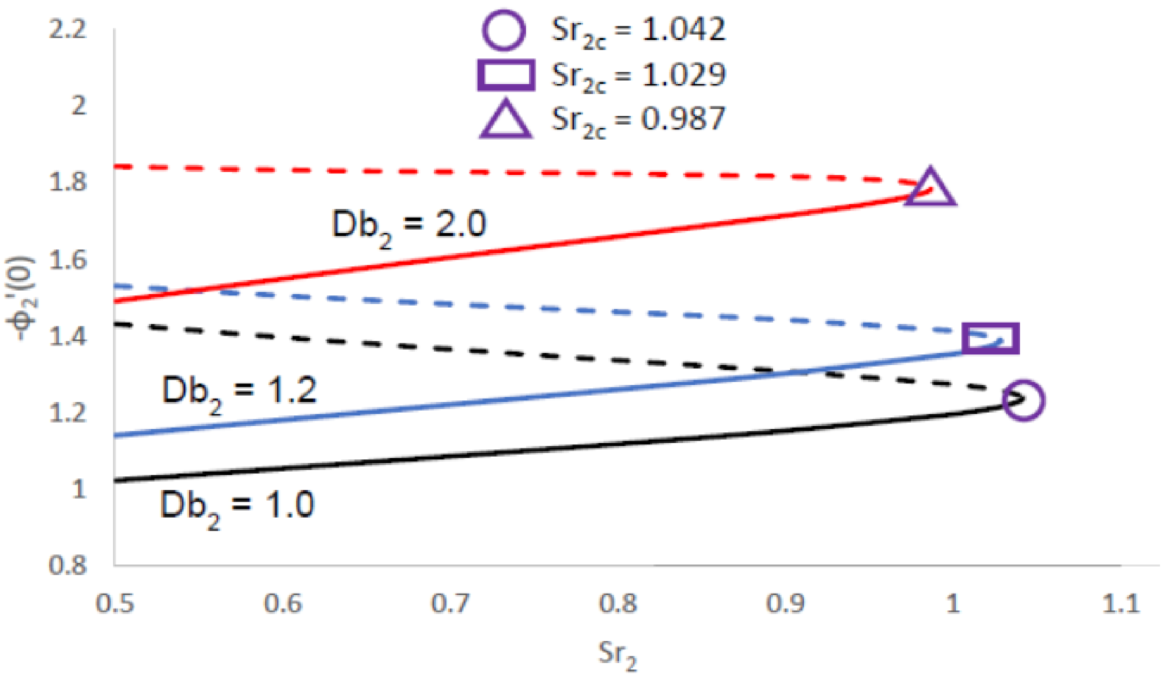

Fig. 5. The variation of local Sherwood number of component 2 against Sr_2 for different values of Db_2

4. Conclusions

The numerical graphics of local Nusselt number and local Sherwood number of the triple diffusive in the Newtonian fluid flow are presented. Hence, the following statements can be written as a conclusions from the Results and Discussion section:

i. When the Dufour number increases, the local Nusselt number will face a decrement. This indicates that if the Dufour parameter is increased, the heat transferred by the mean of conduction increases. In order to ensure most of the heat would be transferred by convection, the Dufour parameter should be decreased.

ii. However, the local Sherwood number increases when the Dufour parameter is increased. Therefore, the mass of Casson fluid to be transferred by convection could be increased by increasing the Dufour number of both components.

This research is restricted to the non-Newtonian Casson fluid, since this type of fluid has higher concentration compared to the Newtonian fluid. This research can be extended to the other non-Newtonian fluid such as Carreau fluid, Maxwell fluid and Eyring-Powell fluid. Moreover, hybrid nanofluids are highly recommended where the specific components of mass C_1 and C_2 can be renamed.

Acknowledgement
The present research was funded by the Fundamental Research Grant Scheme (FRGS/1/2020/STG06/UPM/02/1) from the Ministry of Education (Malaysia).

References
[1] Schlichting, Hermann, and Klaus Gersten. Boundary-layer theory. Springer, 2016.
[2] Lur'e, S. L. "Solutions of boundary-layer equations for a Newtonian fluid on a plate." *Journal of Engineering Physics* 13, no. 3 (1967): 219-219. https://doi.org/10.1007/BF00831482
[3] PATHAK, SK. "LAMINAR BOUNDARY LAYER OVER A FLEXIBLE SURFACE IN OSCILLATORY FLOW. I. NEWTONIAN FLUID." (1975).
[4] KULSHRESHTHA, AK, and JM CARUTHERS. "UNSTEADY MOTION OF A SPHERE IN A NEWTONIAN FLUID: I. VELOCITY BOUNDARY CONDITIONS." *Chemical Engineering Communications* 58, no. 1-6 (1987): 465-486. https://doi.org/10.1080/00986448708911982
[5] Sakiadis, Byron C. "Boundary-layer behavior on continuous solid surfaces: I. Boundary-layer equations for two-dimensional and axisymmetric flow." *AIChE Journal* 7, no. 1 (1961): 26-28. https://doi.org/10.1002/aic.690070108
[6] Swain, B. K., B. C. Parida, S. Kar, and N. Senapati. "Viscous dissipation and joule heating effect on MHD flow and heat transfer past a stretching sheet embedded in a porous medium." *Heliyon* 6, no. 10 (2020). https://doi.org/10.1016/j.heliyon.2020.e05338
[7] Ahmad, Kartini, Zaharah Wahid, and Zahir Hanouf. "Mixed Convection Casson Fluid Flow over an Exponentially Stretching Sheet with Newtonian Heating Effect." *Journal of Mechanic of Continua and Mathematical Sciences, Special Issue* 1 (2019): 203-214. https://doi.org/10.26782/jmcms.2019.03.00020
[8] Sharma, Ram Prakash, and Satyaranjan Mishra. "Analytical approach on magnetohydrodynamic Casson fluid flow past a stretching sheet via Adomian decomposition method." *Heat Transfer* 51, no. 2 (2022): 2155-2164. https://doi.org/10.1002/htj.22393
[9] Rasli, Nurfazila, and Norshafira Ramli. "Magnetohydrodynamic Flow and Heat Transfer Over an Exponentially Stretching/Shrinking Sheet in Ferrofluids." *Pertanika Journal of Science & Technology* 29, no. 3 (2021). https://doi.org/10.47836/pjst.29.3.42
[10] Japili, Nirwana, Haliza Rosali, and Norfifah Bachok. "Slip effect on stagnation point flow and heat transfer over a shrinking/stretching sheet in a porous medium with suction/injection." *Journal of Advanced Research in Fluid Mechanics and Thermal Sciences* 90, no. 2 (2022): 73-89. https://doi.org/10.37934/arfmts.90.2.7389
[11] Yahaya, Rusya Iryanti, Norihan Md Arifin, Fadzilah Md Ali, and Siti Suzilliana Putri Mohamed Isa. "Hybrid Nanofluid Flow with Multiple Slips Over a Permeable Stretching/Shrinking Sheet Embedded in a Porous Medium." *Journal of Advanced Research in Fluid Mechanics and Thermal Sciences* 106, no. 2 (2023): 143-152. https://doi.org/10.37934/arfmts.106.2.143152
[12] Azmi, Hazirah Mohd, Siti Suzilliana Putri Mohamed Isa, and Norihan Md Arifin. "The boundary layer flow, heat and mass transfer beyond an exponentially stretching/shrinking inclined sheet." *CFD Letters* 12, no. 8 (2020): 98-107. https://doi.org/10.37934/cfdl.12.8.98107
[13] Nabwey, Hossam A., S. M. M. El-Kabeir, A. M. Rashad, and M. M. M. Abdou. "Effectiveness of magnetized flow on nanofluid containing gyrotactic micro-organisms over an inclined stretching sheet with viscous dissipation and constant heat flux." *Fluids* 6, no. 7 (2021): 253. https://doi.org/10.3390/fluids6070253

[14] Kanungo, Subhrajit, and Tumbanath Samantara. "Flow And Heat Transfer of Unsteady Two-Phase Boundary Layer Flow Past an Inclined Permeable Stretching Sheet with Electrification of Particles." *CFD Letters* 15, no. 5 (2023): 134-144. https://doi.org/10.37934/cfdl.15.5.134144

[15] Srinivasulu, T., and Shankar Bandari. "MHD, Nonlinear thermal radiation and non-uniform heat source/sink effect on Williamson nanofluid over an inclined stretching sheet." *Malaya J. Matematik (MJM)* 8, no. 3 (2020): 1337-1345. https://doi.org/10.26637/MJM0803/0106

[16] Mishra, Jayaprakash, and Tumbanath Samantara. "Study of Unsteady Two Phase Flow over An Inclined Permeable Stretching Sheet with Effects of Electrification and Radiation." *Journal of Advanced Research in Fluid Mechanics and Thermal Sciences* 97, no. 2 (2022): 26-38. https://doi.org/10.37934/arfmts.97.2.2638

[17] Sneha, K. N., U. S. Mahabaleshwar, and Suvanjan Bhattacharyya. "An effect of thermal radiation on inclined MHD flow in hybrid nanofluids over a stretching/shrinking sheet." *Journal of Thermal Analysis and Calorimetry* 148, no. 7 (2023): 2961-2975. https://doi.org/10.1007/s10973-022-11552-9

[18] Das, U. J. "MHD Boundary Layer Flow of Casson Fluid Past an Inclined Plate in the Presence of Soret/Dufour Effects, Heat Source and First-order Chemical Reaction." *Journal of Scientific Research* 13, no. 3 (2021). https://doi.org/10.3329/jsr.v13i3.52234

[19] Lounis, Selma, Redha Rebhi, Noureddine Hadidi, Giulio Lorenzini, Younes Menni, Houari Ameur, and Nor Azwadi Che Sidik. "Thermo-Solutal Convection of Carreau-Yasuda Non-Newtonian Fluids in Inclined Square Cavities Under Dufour and Soret Impacts." *CFD Letters* 14, no. 3 (2022): 96-118. https://doi.org/10.37934/cfdl.14.3.96118

[20] Sekhar, P. Raja, S. Sreedhar, S. Mohammed Ibrahim, and P. Vijaya Kumar. "Radiative Heat Source Fluid Flow of MHD Casson Nanofluid over A Non-Linear Inclined Surface with Soret and Dufour Effects." *CFD Letters* 15, no. 7 (2023): 42-60. https://doi.org/10.37934/cfdl.15.7.4260

[21] Manjunatha, N., Umair Khan, Samia Elattar, Sayed M. Eldin, Jasgurpreet Singh Chohan, R. Sumithra, and K. Sarada. "Onset of triple-diffusive convective stability in the presence of a heat source and temperature gradients: An exact method." *AIMS Mathematics* 8, no. 6 (2023): 13432-13453. https://doi.org/10.3934/math.2023681

[22] Yellamma, Manjunatha Narayanappa, Ramalingam Udhayakumar, Barakah Almarri, Sumithra Ramakrishna, and Ahmed M. Elshenhab. "The Impact of Heat Source and Temperature Gradient on Brinkman–Bènard Triple-Diffusive Magneto-Marangoni Convection in a Two-Layer System." *Symmetry* 15, no. 3 (2023): 644. https://doi.org/10.3390/sym15030644

[23] Balaji, Varalakshmi K., Manjunatha Narayanappa, Ramalingam Udhayakumar, Ghada AlNemer, Sumithra Ramakrishna, and Gangadharaih Yeliyur Honnappa. "Effects of LTNE on Two-Component Convective Instability in a Composite System with Thermal Gradient and Heat Source." Mathematics 11, no. 20 (2023): 4282. https://doi.org/10.3390/math11204282

[24] Manjunatha, N., Yellamma, R. Sumithra, K. M. Yogeesha, Rajesh Kumar, and R. Naveen Kumar. "Roles and impacts of heat source/sink and magnetic field on non-Darcy three-component Marangoni convection in a two-layer structure." *International Journal of Modern Physics B* 37, no. 19 (2023): 2350186. https://doi.org/10.1142/S0217979223501862

[25] Manjunatha, N., Yellamma, R. Sumithra, Amit Verma, RJ Punith Gowda, and J. Madhu. "The impact of the heat source/sink on triple component magneto-convection in superposed porous and fluid system." *Modern Physics Letters B* 38, no. 07 (2024): 2450020. https://doi.org/10.1142/S0217984924500209

[26] Archana, M., M. G. Reddy, B. J. Gireesha, B. C. Prasannakumara, and S. A. Shehzad. "Triple diffusive flow of nanofluid with buoyancy forces and nonlinear thermal radiation over a horizontal plate." *Heat Transfer—Asian Research* 47, no. 8 (2018): 957-973. https://doi.org/10.1002/htj.21360

[27] Junoh, Mohamad Mustaqim, Nursyahanis Abdullah, and Fadzilah Md Ali. "Dual Solutions of MHD Stagnation Slip Flow Past a Permeable Plate." *Journal of Advanced Research in Fluid Mechanics and Thermal Sciences* 80, no. 1 (2021): 137-146. https://doi.org/10.37934/arfmts.80.1.137146

[28] Ali, Fadzilah Md, Amira Natasya Azizan Khamat, and Mohamad Mustaqim Junoh. "Dual solutions in mixed convection stagnation-point flow over a vertical stretching sheet with external magnetic field and radiation effect." *Journal of Advanced Research in Fluid Mechanics and Thermal Sciences* 80, no. 2 (2021): 22-32. https://doi.org/10.37934/arfmts.80.2.2232

[29] Zainal, Nurul Amira, Roslinda Nazar, Kohilavani Naganthran, and Ioan Pop. "Stability analysis of unsteady hybrid nanofluid flow past a permeable stretching/shrinking cylinder." *Journal of Advanced Research in Fluid Mechanics and Thermal Sciences* 86, no. 1 (2021): 64-75. https://doi.org/10.37934/arfmts.86.1.6475

[30] Siti Suzilliana Putri Mohamed Isa, Nanthini Balakrishnan, Nurul Syuhada Ismail, Norihan Md. Arifin, & Fadzilah Md Ali. The Velocity, Temperature and Concentration Profiles for Triple Diffusive Casson Fluid Flow Subjected to the Soret-Dufour Parameters. *CFD Letters*, 16, no. 3 (2023): 15–27. https://doi.org/10.37934/cfdl.16.3.1527

[31] Parvin, Shahanaz, Siti Suzilliana Putri Mohamed Isa, Fuad S. Al-Duais, Syed M. Hussain, Wasim Jamshed, Rabia Safdar, and Mohamed R. Eid. "The flow, thermal and mass properties of Soret-Dufour model of magnetized

Maxwell nanofluid flow over a shrinkage inclined surface." *PLoS One* 17, no. 4 (2022): e0267148. https://doi.org/10.1371/journal.pone.0267148
[32] Parvin, S., S. S. P. M. Isa, N. M. Arifin, and F. M. Ali. "Soret-Dufour impacts on inclined magnetic Casson fluid flow." *Magnetohydrodynamics* (0024-998X) 57, no. 3 (2021). https://doi.org/10.22364/mhd.57.3.4
[33] Parvin, Shahanaz, Siti Suzilliana Putri Mohamed Isa, Norihan Md Arifin, and Fadzilah Md Ali. "Soret and Dufour effects on magneto-hydrodynamics Newtonian fluid flow beyond a stretching/shrinking sheet." *CFD Letters* 12, no. 8 (2020): 85-97.